Combustion, Explosion, and Shock Waves, Vol. 46, No. 4, pp. 371–379, 2010

Unsteady Modes of Filtration Combustion

A. N. Firsov,[1] N. I. Ozerkovskaya,[2] and K. G. Shkadinskii[1] UDC 536.46

Translated from *Fizika Goreniya i Vzryva*, Vol. 46, No. 4, pp. 3–12, July–August, 2010.
Original article submitted February 6, 2009.

Unsteady modes of filtration combustion are studied with the use of a three-dimensional mathematical model. The model describes exothermic chemical interaction of condensed systems with active gases and formation of solid products. Unsteadiness of the filtration combustion modes is caused by instability of the plane combustion front. Formation of the periodic structure of the front of combustion of porous cylindrical samples with different cross-sectional shapes is studied. It is demonstrated that different periodic regimes of combustion-front propagation can occur under conditions of instability of the plane combustion front and deficit of the active gas mass inside the pores, depending on the cross-sectional shape of cylindrical samples and various methods of heat and mass transfer between the sample and the ambient gas medium. Periodic regimes of oscillatory (volume and surface) combustion for samples with a circular cross section, spinning mode for samples with a ring-shaped cross section, and complicated periodic regimes for samples with a rectangular cross section are obtained.

Key words: filtration combustion, front instability, mathematical modeling.

INTRODUCTION

The filtration combustion theory has been lately developed on the basis of new data on exothermic chemical interaction of porous condensed systems with active gases and formation of solid products (see the reviews in [1, 2]). The mathematical description of this process was reduced to rather complicated nonlinear systems of differential equations that characterize macrokinetics of chemical interaction and processes of heat and mass transfer in porous media. At the initial stage, mathematical modeling was restricted to studying one-dimensional processes. The transition to two-dimensional mathematical models [3, 4] made it possible to identify the regions of existence of plane and surface modes of filtration combustion. Effects of stimulating of chemical conversion in individual zones of the reacting medium volume owing to specific features of heat- and mass-transfer organization were found. An adequate description of many real unsteady processes, however, requires the analysis to be performed on the basis of three-dimensional models of filtration combustion. Unfortunately, construction of these models is restricted both by the level of computational technology and by the lack of effective approximate methods of mathematical modeling. A three-dimensional model of gasless combustion with unsteady combustion modes found near the stability boundary was first considered in [5]. A comprehensive analysis of this model was performed in [6].

The present work is aimed at studying three-dimensional unsteady frontal regimes arising in the region of instability of a plane quasi-steady filtration combustion front [7]. Combustion of cylindrical samples with different cross-sectional shapes is considered.

MATHEMATICAL MODEL

The process of chemical interaction of a porous condensed sample with a gas and formation of a solid product follows the scheme

$$\mu_g \mathrm{R}_g + \mu_c \mathrm{R}_c \to \mu_p \mathrm{R}_p,$$

[1] Institute of Problems of Chemical Physics, Russian Academy of Sciences, Chernogolovka 142432; shkad@ficp.ac.ru.
[2] Institute of Structural Macrokinetics and Material Science, Chernogolovka 142432.

0010-5082/10/4604-0371

where μ_g, μ_c, and μ_p are stoichiometric coefficients, R_g and R_c are the gaseous and condensed reagents, and R_p is the product. This process is described by a mathematical model with dimensionless variables, which includes:
the law of conservation of mass of the gas

$$\frac{\partial(\rho m)}{\partial\tau} + \mathrm{div}(\rho m \boldsymbol{V}) = -\mu_\eta \rho_\eta \frac{\partial\eta}{\partial\tau}, \tag{1}$$

the Darcy equation determining the gas motion velocity

$$\boldsymbol{V} = -K_f(m)\mathrm{grad}P, \tag{2}$$

the equation of state of the gas

$$P = \rho(1+\beta\theta), \tag{3}$$

the law of conservation of energy (enthalpy)

$$\frac{\partial H}{\partial\tau} = \mathrm{div}\left(\lambda(m)\nabla\theta - c_g\rho m\boldsymbol{V}\frac{1+\beta\theta}{\beta}\right),$$

$$H = (c_g\rho m + c_\eta\rho_\eta(1+\mu_\eta\eta))\frac{1+\beta\theta}{\beta} + \rho_\eta\frac{1-\eta}{\gamma}, \tag{4}$$

$$\rho_\eta = (1-m)\nu,$$

and the equation of chemical interaction macrokinetics

$$\frac{\partial\eta}{\partial\tau} = \gamma(1-\eta)\exp\left(\frac{\theta}{1+\beta\theta}\right)\frac{P}{P+\delta}. \tag{5}$$

The boundary conditions determine the conditions of heat and mass transfer between the sample and the ambient gas medium. Boundary conditions of the following form can be imposed on various parts of the side surface ∂S_{bn} or on the entire surface S_{bn} of the sample:
for $\tau > 0$ and $A \in S_{bn}$,

$$\theta(A,\tau) = \theta_w, \quad P(A,\tau) = P_{bn},$$
$$\frac{\partial\theta(A,\tau)}{\partial\boldsymbol{n}} = 0, \quad \frac{\partial P(A,\tau)}{\partial\boldsymbol{n}} = 0;$$

for $\tau > 0$ and $A \in \partial S_{bn}$,

$$\lambda(m)\frac{\partial\theta(A,\tau)}{\partial\boldsymbol{n}} = \begin{cases} c_g\rho\boldsymbol{V}(\theta(A,\tau)-\theta_{bn}) \text{ for } P_{\partial S} < P_{bn}, \\ 0 \quad \text{otherwise;} \end{cases}$$

for $\tau > 0$ and $A \in \partial S_{bn}$,

$$\lambda(m)\frac{\partial\theta(A,\tau)}{\partial\boldsymbol{n}} = \alpha_{\partial S}(\theta(A,\tau)-\theta_{bn}).$$

The state of the physical fields inside the sample (temperature, pressure, conversion depth, and gas density) at the initial time is determined by the initial conditions:

$$\theta = \theta_0, \quad P = P_0, \quad \eta = \eta_0, \quad \rho_0 = P_0/(1+\beta\theta_0).$$

The transition to dimensionless parameters is performed by the following formulas:

$$c_g = c_{g0}/c_*, \quad c_\eta = c_{c0}/c_*, \quad \rho = \rho_g/\rho_*,$$
$$\rho_\eta = \rho_{c0}\nu(1-m)/\rho_*, \quad \lambda_\eta = \lambda_{c0}/\lambda_*,$$
$$\lambda_g = \lambda_{g0}/\lambda_*, \quad \lambda(m) = m\lambda_g + (1-m)\nu\lambda_\eta,$$
$$\mu_\eta = \frac{\mu_g M_g}{\mu_c M_c}, \quad a = \frac{\lambda_*}{c_*\rho_*}, \quad \alpha_{\partial S} = \frac{\alpha x_*}{\lambda_{c0}},$$
$$K_f(m) = \frac{k_f P_*}{a}, \ \gamma = \frac{RT_*^2}{E(T_* - T_0)}, \ \beta = \frac{RT_*}{E},$$
$$x_*^2 = at_*, \ t_* = \frac{\gamma}{k_0\exp(-E/RT_*)}, \ P_* = \frac{RT_*\rho_*}{M_g},$$
$$T_* \approx T_0 + \frac{Q}{c_{c0}}, \ c_* = c_{c0}, \ \lambda_* = \lambda_{c0}, \ \rho_* = \rho_{c0},$$
$$\theta = \frac{T - T_*}{RT_*^2/E}, \quad \eta = \frac{C_0 - C}{C_0}, \quad P = p/P_*,$$
$$\boldsymbol{V} = \boldsymbol{U}t_*/x_*, \quad \tau = t/t_*, \quad \delta = 10^{-6}.$$

In these equations, the dimensional quantities are the medium temperature T, the gas pressure p, the density ρ, the concentration of the condensed reagent C, the activation energy E, the pre-exponent k_0, the thermal effect of the reaction Q, the velocity vector of gas motion $\boldsymbol{U}$, the filtration coefficient k_f, the heat capacity c, the thermal conductivity λ, the thermal diffusivity a, the heat loss coefficient α, the gas constant R, and the molecular mass M. The dimensionless quantities are the stoichiometric coefficient μ_η, the fraction of the condensed phase in a unit volume of the medium ν, the porosity of the medium (fraction of the gas phase in a unit volume of the medium) m, a small parameter characterizing the weak dependence of the reaction rate on the gas pressure except for the low-pressure region δ, and the high-temperature pulse θ_w. The subscripts refer to the initial quantities (0), the quantities used for normalization $(*)$, the gas (g), the condensed non-porous medium (c), the dimensionless density of the condensed porous medium (η), and the ambient medium (bn). The reference quantities are characteristic combustion time t_* and the characteristic size of the chemical reaction zone x_*. The combustion theory predicts that $t_* \sim a\gamma^2/u^2$ and $x_* \sim a\gamma/u$ (where u is the burning rate). For the class of systems considered (porous reagent + active gas $\rightarrow$ solid product [8]), we obtain $t_* \approx 4\cdot10^{-4}$–$3\cdot10^{-2}$ sec and $x_* \approx 2\cdot10^{-3}$–$3\cdot10^{-2}$ cm. It should be noted that these data are approximate because macrokinetics of chemical interaction under combustion conditions has not been studied to a sufficient extent.

The three-dimensional mathematical model (1)–(5) with appropriate boundary and initial conditions was studied by the method of variable directions [9] with nonuniform grids adapting to solution singularities [10]. As the combustion front propagated over the examined sample, the computational domain was increased under certain conditions from the side of the reagents, while some part of the computational domain from the side of the combustion products was deleted. This procedure made it possible to study the dynamics of the flow reaching steady combustion modes. Using this approach, we actually simulate operation of a continuous displacement reactor.

ANALYSIS OF RESULTS

The basic features of combustion modes of porous condensed systems in an active gas medium are determined by chemical interaction, heat transfer, and gas motion. An intense chemical reaction occurs only if all components participating in this reaction are available and are heated to a high temperature. It is important that complete conversion of the condensed medium requires such an amount of the gaseous reagent that its mass is commensurable with the mass of the initial condensed substance. The mass of the gas in the sample depends on the gas pressure and pore volume. Formation of the combustion product as a result of the chemical reaction involves heat release, an increase in temperature in the reaction zone, consumption of the gas, a decrease in the gas pressure, and the emergence of a pressure gradient inducing gas filtration into the chemical reaction zone from the neighboring areas of the porous substance and from the ambient gas medium (if the surface of the porous medium is permeable for the gas). The burning sample experiences interrelated spatial-temporal reconstruction of the fields of temperature, pressure, gas velocity, and depth of conversion. The field of the conversion depth, which displays the result of chemical interaction, provides the best idea about the complicated multidimensional dynamics of the geometry of the chemical reaction zone, which controls filtration processes.

Instability of the quasi-steady frontal regime of filtration combustion [7] complicates the combustion process. When a plane quasi-steady combustion front loses its stability, new non-one-dimensional periodic stable combustion modes appear for parameters near the stability boundary. The evolution of these new modes is determined by the governing parameters of the mathematical model. The three-dimensional mathematical model (1)–(5) contains three important factors of the frontal regime of exothermic chemical conversion: macrokinetics of chemical interaction exponentially depending on temperature (corresponding to the energy-release rate); filtration transport of the gaseous reagent into the active chemical reaction zone, which is nonlinear, but similar to diffusion transport in diffusion flame models; heat-transfer mechanism. Here, we can consider an analog of the Lewis criterion characterizing the relations between the active gaseous reagent transport properties and thermal diffusivity. Therefore, a situation similar to the thermal diffusion flame front is expected in terms of stability of the frontal regime of exothermic conversion, though the situation is expected to be substantially more nonlinear. In the limiting cases, for instance, in the absence of permeability (analog of "gasless" combustion), spinning combustion modes are expected to exist. At high filtration coefficients (analog of the thermal diffusion flame with a high Lewis number), the front is expected to have a cellular structure. Certainly, other versatile nonlinear combustion modes are also possible, because the geometric shape of the burning samples and the conditions of interaction with the ambient medium are also important factors in addition to those three indicated above.

Let us first consider the results of studying combustion of porous cylindrical samples in an active gas medium, with the heat and mass exchange with the ambient medium proceeding through the sample surface. The process of combustion is initiated from the lower end face by a high-temperature impulse θ_w. In our calculations, the thermophysical parameters of the medium ($c_g = 0.5$, $\lambda_g = 5.0 \cdot 10^{-3}$, $\mu_\eta = 0.3$, $m = 0.5$, $c_\eta = 1.0$, and $\lambda = 0.5$) are constant; the varied parameters were γ, β, $P_0 = P_{bn}$, K_f, and θ_0, the sample shape, and the conditions of interaction with the ambient medium.

The physical fields (temperature, pressure, and conversion depth) were visualized in a plane cross section of the sample with identification of the dynamics of isolines of the corresponding fields. This procedure provided information about the gradients responsible for the heat and gas-mass fluxes. It should be noted that visual information about the internal processes in the sample is unavailable in real physical experiments where the initial and final products are condensed.

Let us consider a periodic process of combustion of a cylindrical sample (height $h = 1200$ and radius $r = 100$) with a gas-permeable side surface through which heat transfer proceeds in accordance with Newton's law with the coefficient $\alpha_{\partial S} = 2.5 \cdot 10^{-2}$. The ambient pressure here is chosen to be $P_{bn} = 5 \cdot 10^{-3} = P_0$; it is lower than the stoichiometric value $P_{st} = 3.6 \cdot 10^{-2}$ (at which the amount of the intraporous active gas is

sufficient for stoichiometric conversion of the porous medium); the filtration coefficient is $K_f = 9.2 \cdot 10^3$; the parameters have the values $\gamma = 0.06$, $\beta = 0.11$, $\theta_0 = \theta_{bn} = -8.0$, and $\theta_w = 1.0$. Figure 1 shows the isolines of the conversion depth, temperature, and pressure in the plane axial cross section of the cylinder, which were obtained at consecutive times. They determine the dynamics of the front structure in one period of the combustion process. Isolines 1 and 2 ($\eta = 0.1$ and 0.9) characterize the dynamics of the active chemical conversion zone. Isotherms 3–5 ($\theta = -5.0$, -1.0, and 1.0) show the dynamics of the thermal structure of the combustion front. Isobars 6 and 7 ($P = 4.9 \cdot 10^{-3}$ and $5 \cdot 10^{-4}$) characterize the dynamics of filtration fluxes and the zone of intense absorption of the active gaseous species. These figures illustrate the dynamics of the first period of combustion front propagation after combustion initiation by a high-temperature source on the surface $X = 0$. After ignition (see Fig. 1a), a complicated axisymmetric dynamic structure of the front is formed and moves in the X direction; the characteristic of the leading zone experiences periodic changes over the radius. The cross-section plane has two (by virtue of axial symmetry) subsurface high-temperature regions with the conversion depth close to unity (see isoline 2, $\eta = 0.9$, in Fig. 1a). They are separated by the region of the product with the conversion depth smaller than unity. The active gas is almost completely consumed in this region (see isobar 7), and the gas incoming from the opposite side through the filtration mechanism is consumed in the chemical reaction in the leading zone of the front (isotherm 4; $\theta = -1.0$). Because of heat losses on the side surface of the sample, the temperature in the subsurface region has a reduced value (isotherm 3; $\theta = -5.0$), practically no combustion products are formed here at the initial time, and the gas is not consumed. The pressure field is reconstructed because the filtration gas flow moves through the subsurface layers inward the cylinder to the high-temperature zone (isotherm 4; $\theta = -1.0$), in addition to the averaged opposing filtration (isobar 6; $P = 4.9 \cdot 10^{-3}$), thus, increasing the chemical reaction rate and, hence, heat release in this zone. The high-temperature spots grow in size, and they are partly shifted to the axial region of the medium, finalizing their exothermic chemical conversion there.

The leading part of the spots tends to go onto the side surface of the samples, because more favorable thermal and filtration conditions for chemical conversion are formed near this surface. Before the spots reach the sample surface, however, conditions for initiation and vigorous proceeding of the chemical reaction (isotherm 5 in Fig. 1b) with complete conversion depth are formed on this surface owing to availability of a sufficient amount of the gaseous reagent. Reconstruction of conversion depth, temperature, and pressure fields is illustrated by the isolines in Fig. 1b.

The chemical reaction covers greater and greater areas on the side surface of the sample with time; as a result, the main and surface spots are united, and the combustion front propagates from the sample surface in the cocurrent filtration mode (see Fig. 1c). Both the front of exothermic conversion moving upstream over the fresh porous medium and the "decaying" front of afterburning of the subsurface non-reacted medium are observed here. The temperature field is reconstructed in accordance with conductive heat transfer and also convective heat transfer due to the changed gas velocity field under conditions of external heat losses. New spots are formed on the leading front in the subsurface zone (there is a sufficient amount of the active gas here, and the heat losses affect only the subsurface zone of the porous medium).

All these processes form a complicated non-one-dimensional combustion mode periodically repeated in time. The combustion products display periodic incomplete burning in subsurface layers (see Fig. 1d, which shows the conversion depth field). It should be noted that some areas of the combustion front are supplied through opposing filtration, and the other areas are supplied through cocurrent filtration.

The dynamics of formation and propagation of the non-one-dimensional structure of the combustion front changes if the filtration coefficient is increased to $K_f = 9.8 \cdot 10^3$ with the other parameters of the mathematical model being unchanged. In this case, because of the increase in the filtration rate, there is no combustion front passing from the side surface toward the upper parts of the internal spots of the sample. Here, the subsurface fluctuations of the conversion depth are much more noticeable (the product is formed with more incomplete burning than at $K_f = 9.2 \cdot 10^3$).

A similar combustion mode is observed in the case of porous cylindrical samples of tubular "geometry" with the inner surface of the tube being insulated in terms of heat and mass transfer and with the outer surface being permeable for the gas.

If the side surface of the cylindrical sample (height $h = 400$ and radius $r = 100$) is impermeable for the gas, then the subsurface combustion mode is observed under conditions of external heat losses ($\alpha_{\partial S} = 1.0 \cdot 10^2$) and opposing filtration of the gas through the open upper end face of the sample ($P_{bn} = 1.0 \cdot 10^{-2} = P_0$, $K_f = 1.0 \cdot 10^4$, $\gamma = 0.06$, $\beta = 0.11$, $\theta_0 = \theta_{bn} = -8$, and $\theta_w = 1$) (Fig. 2). Here, the front structure is characterized by the conversion depth isolines $\eta = 0.25$ and

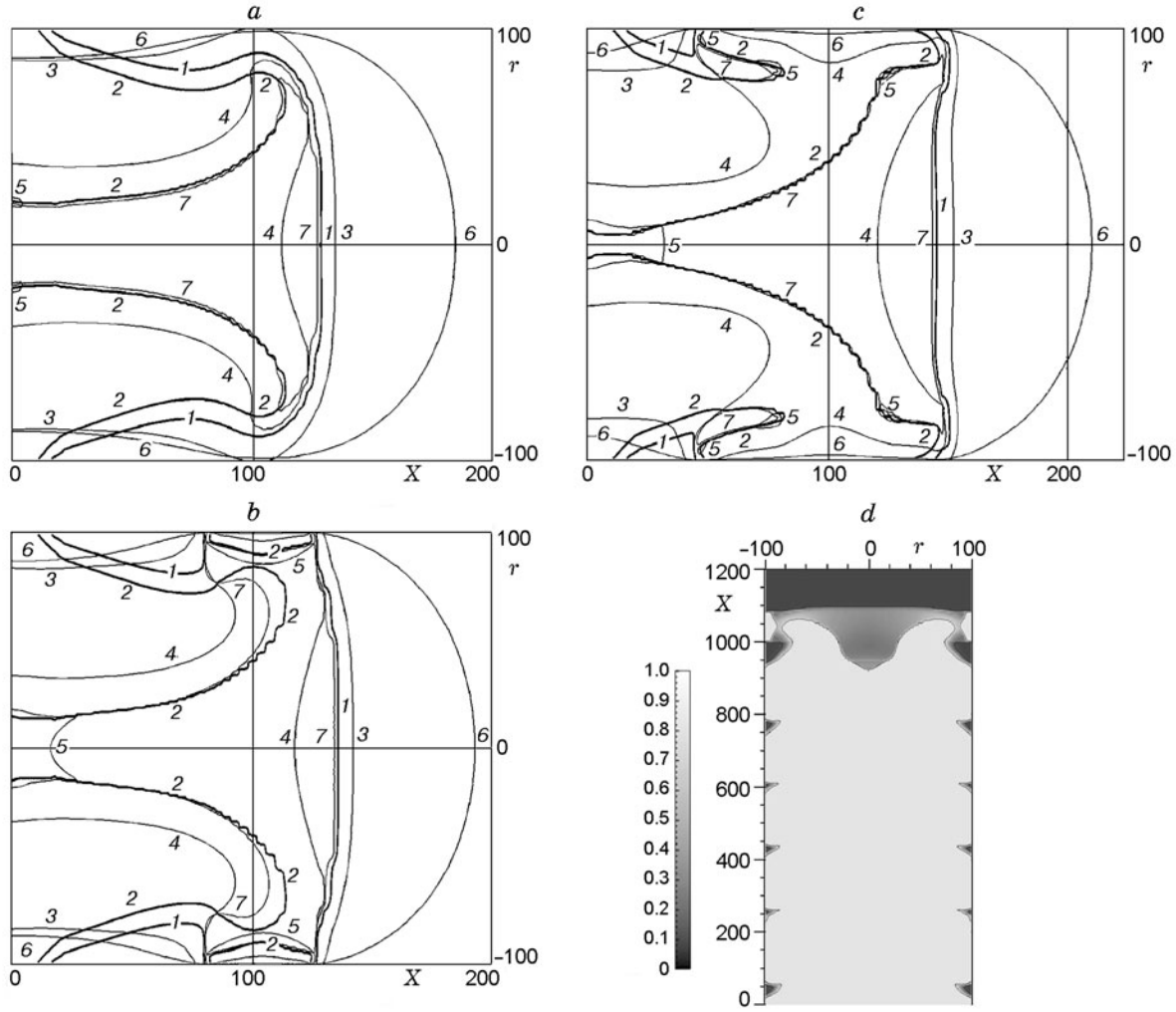

Fig. 1. Nonlinear dynamics of formation of the non-one-dimensional structure of the front of filtration combustion of a porous cylindrical sample and its propagation over the sample with incomplete subsurface burning: isolines $\eta = 0.1$ (1) and 0.9 (2), $\theta = 5.0$ (3), -1.0 (4), and 1.0 (5), and $P = 4.9 \cdot 10^{-3}$ (6) and $5.0 \cdot 10^{-4}$ (7).

0.99, isotherms $\theta = -3.0$, -1.0, and 0.5, and isobars $P = 6.5 \cdot 10^{-3}$ and $3.0 \cdot 10^{-4}$. It should be noted that the heat losses from the side surface of the sample reduce the temperature in the subsurface layer so that no combustion products are formed there, and an additional channel for gas motion to active chemical conversion zones remote from the side surface is formed. Significant incompleteness of conversion is typical for the interior region around the cylinder axis. The reason is almost complete consumption of the active gas incoming from the upper end face in the leading zone of the combustion front. As the front approaches the open end, however, the conversion depth reaches the value of unity. At this stage, there appears an afterburning front, which propagates in the opposite direction and is supported by the cocurrent gas flow through the final reaction products being formed. This bifurcation of the combustion front was observed earlier in the one-dimensional description.

In the range of parameters where the plane quasi-steady front of filtration combustion becomes unstable, there may appear a new stable periodic regime where the chemical reaction zone is focused in a small (as compared with the sample diameter) spot. This spot moves along a spiral on the surface of the burning system and penetrates inward the sample to a small depth. This regime was observed in experiments with combustion of metals (titanium, tantalum, hafnium, etc.) in the nitrogen medium and was called the spinning mode [8]. A specific feature of this mode is spot motion over a pre-heated layer due to the process of combustion at the previous coil. Note that the resultant stable periodic front is not axisymmetric, though the sample and the parameters characterizing its initial state possess symmetry of this type.

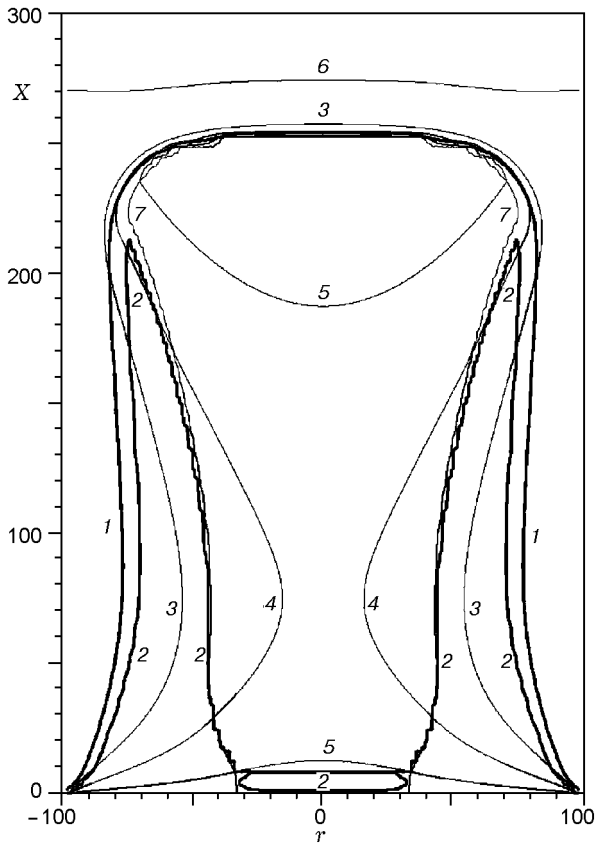

Fig. 2. Subsurface mode of filtration combustion of a porous cylindrical sample: isolines $\eta = 0.25$ (1) and 0.99 (2), $\theta = -3.0$ (3), -1.0 (4), and 0.5 (5), and $P = 6.5 \cdot 10^{-3}$ (6) and $3.0 \cdot 10^{-4}$ (7).

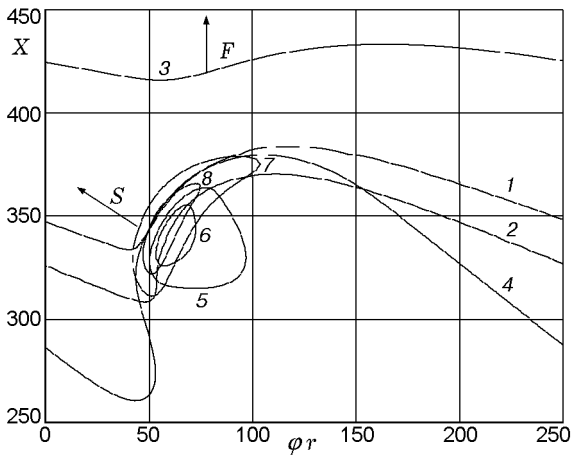

Fig. 3. Structure of the spinning front of filtration combustion of a porous cylindrical tube with the inner surface of the tube being insulated in terms of heat and mass transfer and with the outer surface being permeable for the gas: isolines $\eta = 0.1$ (1) and 0.9 (2), $\theta = -0.8$ (3), -1.75 (4), 0 (5), and 0.5 (6), and $P = 4.9 \cdot 10^{-3}$ (7) and $4.95 \cdot 10^{-3}$ (8).

For the mathematical model parameters $\gamma = 0.085$, $\beta = 0.09$, $\theta_0 = \theta_{bn} = -10$, $\theta_w = 1$, $\mu_\eta = 0.3$, $m = 0.5$, $P_{bn} = 5 \cdot 10^{-3} = P_0$, and $K_f = 5.0 \cdot 10^3$, the spinning mode of filtration combustion was obtained in a sample shaped as a thin tube (height $h = 500$, radius $r = 40$, and tube wall thickness $\Delta r = 0.2$) with the inner surface of the tube being insulated in terms of heat and mass transfer and with the outer surface being permeable for the gas. Figure 3 shows the isolines of the physical fields (isolines of conversion depth $\eta = 0.1$ and 0.9, isotherms $\theta = -8.0$, -1.75, 0, and 0.5, and isobars $P = 4.9 \cdot 10^{-3}$ and $4.95 \cdot 10^{-3}$), which characterize the combustion front structure (spin). The arrows indicate the direction of propagation of the high-temperature spot along the heated layer (S) and the direction of motion of the averaged front (F). The complicated dynamics of stabilization of the spinning regime is worth noting. Before reaching a steady spinning mode, the combustion front after initiation propagates in the pulsed mode (typical for thin one-dimensional samples) and then in the multispot mode (with random dynamics of spot motion).

It is well known that the dynamics of frontal exothermic chemical conversion in the region of instability of the plane front depends on the geometry (cross-sectional topology) of cylindrical samples. Complicated multi-dimensional regimes are observed during filtration combustion of porous condensed samples with a rectangular cross section. Let us consider the results of a three-dimensional numerical analysis of filtration combustion of a flat plate. Its Y size is much smaller than its X and Z sizes ($L_X = 400$, $L_Y = 2$, and $L_Z = 335$), $\gamma = 0.06$, $\beta = 0.11$, $\theta_0 = \theta_{bn} = -8$, and $\theta_w = 1$. The ambient pressure $P_{bn} = 2.5 \cdot 10^{-3}$ is lower than the stoichiometric value $P_{st} = 3.6 \cdot 10^{-2}$, the filtration coefficient is $K_f = 5.0 \cdot 10^4$, the lower end face of the plate is ignited by a high-temperature source ($\theta_w = 0$), and the upper end face is permeable for the gas. The other (side) faces of the plate are impermeable for the gas. The XZ faces are thermally insulated, and the XY faces allow heat transfer by Newton's law with the coefficient $\alpha_{\partial S} = 100$.

Figures 4a and 4b show some fragments of the dynamics of development of unsteady combustion of such a plate. Note that such a quasi-two-dimensional porous medium allows a better approximation of the mathematical model of the process and, hence, a more detailed analysis of the process. The position of a comparatively narrow conversion front is characterized by the isoline $\eta = 0.5$, while the position of the thermal front

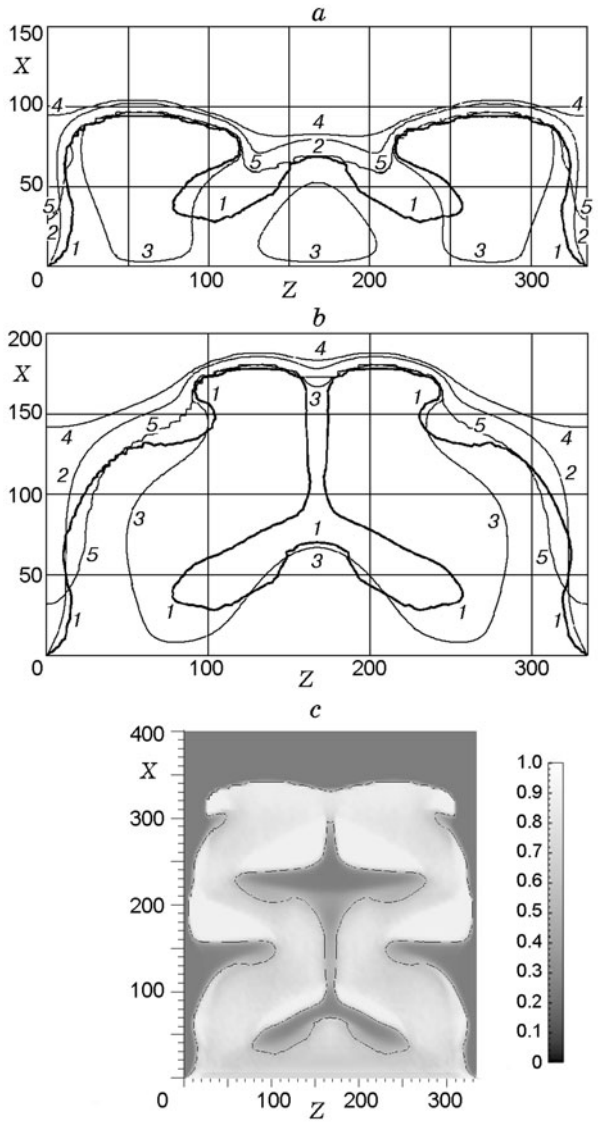

Fig. 4. Dynamics of development of unsteady filtration combustion of a porous plate with a gas-impermeable side surface and gas-permeable upper end face: the XZ faces are thermally insulated, and the XY faces allow heat transfer by Newton's law with the coefficient $\alpha_{\partial S} = 100.0$; isolines $\eta = 0.5$ (1), $\theta = -0.5$ (2) and -0.1 (3), and $P = 2.0 \cdot 10^{-3}$ (4) and $2.0 \cdot 10^{-4}$ (5).

is characterized by the isotherms $\theta = -5.0$ and -0.1 and by the isobars $P = 2.0 \cdot 10^{-3}$ and $2.0 \cdot 10^{-4}$. Three spots are formed after ignition. The spot in the middle fails because the thermal and filtration combustion for its development are deteriorated owing to enhancement of chemical conversion of subsurface layers whose complex interaction is manifested in changes in the temperature, pressure, and conversion depth fields shown in Fig. 4b. The spots move toward each other up to the plate center (see Figs. 4a and 4b), propagate in the Y direction in the central part of the plate, move to the plate edges, and continue to move along the edges. After that, the process of spot motion is repeated again. As the combustion front approaches the open surface (see Fig. 4c, which shows the conversion depth field), the spots merge, and a plane front is formed and propagates further.

If the upper end face of the sample is impermeable for the ambient gas, then the chemical reaction can consume only the gas located in the pores. This amount of the gas is insufficient for the above-described pattern to be repeated; as the combustion front approaches the closed surface, the dynamics similar to that illustrated in Figs. 4a and 4b is first observed, then it changes, and combustion is terminated because of the lack of the gaseous reagent.

Note that the dynamics of combustion-front propagation in plates is also asymmetric, despite the initial symmetry (both of the sample and of the parameters characterizing its initial state).

For large sample thicknesses ($L_X = 600$, $L_Y = 250$, and $L_Z = 250$), a more complicated non-one-dimensional regime of filtration combustion of porous condensed compositions ($\gamma = 0.06$, $\beta = 0.11$, $\theta_0 = \theta_{bn} = -8.0$, $\theta_w = 1.0$, $K_f = 9.2 \cdot 10^3$, and $P_{bn} = P_0 = 5 \cdot 10^{-3}$) with heat and mass exchange with the ambient medium (the heat-transfer coefficient is the same for all faces, $\alpha_{\partial S} = 2.5 \cdot 10^{-2}$; the side faces and the upper end face are permeable for the gas) is observed.

This regime is characterized by periodic emergence of spots on the sample faces (Fig. 5a), their splitting into two spots moving toward the edges (Fig. 5b), their merging on the edges, translational motion along the edges, and splitting again into two spots moving toward the face centers (Fig. 5c). The dynamics of the temperature fields in the sample is illustrated in Fig. 5. Similar non-one-dimensional regimes of unsteady combustion of ferro-zirconium thermite samples with a rectangular cross section were studied in [11]. Conducting a real experiment, the observer obtains only such an external pattern of the complicated frontal process proceeding inside the sample volume. The mathematical model allows the researcher to "peep" inside the volume and see the nonlinear dynamics of the front similar to that shown in Fig. 4.

CONCLUSIONS

Stable frontal modes of exothermic chemical conversion allow organizing self-sustained energy release

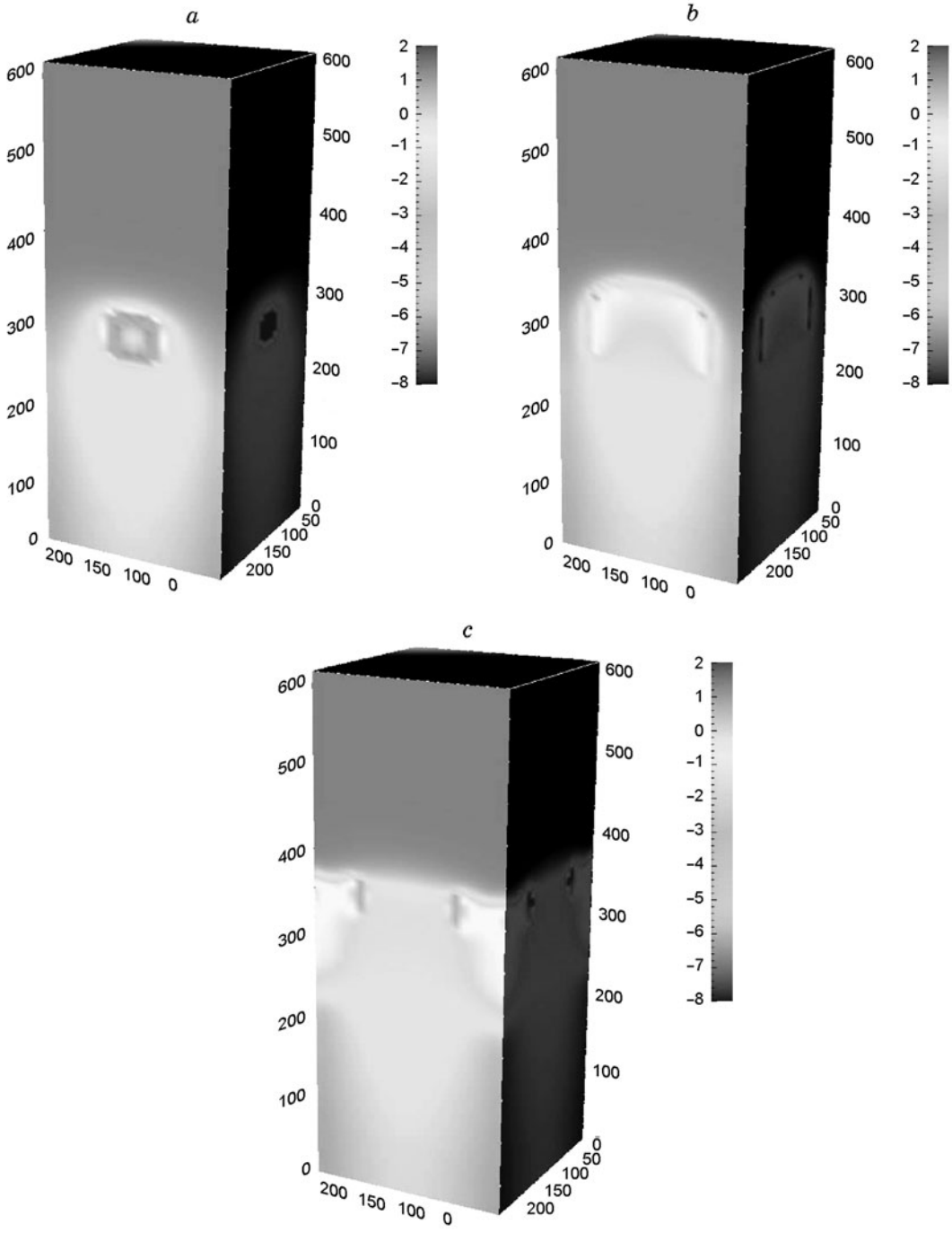

Fig. 5. Periodic non-one-dimensional regime of filtration combustion of a sample with a rectangular cross section under conditions of heat and mass exchange with an active gas medium.

and obtaining the final product by means of local initiation of the process. Interaction with the ambient medium can distort the plane front geometry and lead to frontal regimes with incomplete conversion and subsequent afterburning. Intense interaction with the ambient medium can give rise to critical phenomena, such as breakdown of the frontal mode of flame propagation (its extinction). An attempt to ensure a plane frontal mode under conditions of its instability leads to the emergence of additional options of front propagation:

spinning regimes, cellular structures with complicated geometry and composition of the products, etc. It is known that the product structure and its properties depend on the conditions and dynamics of obtaining this product. Materials and articles with a wide range of properties are obtained by high-temperature synthesis. The results presented above reveal the existence of new technological options with the use of frontal regimes for synthesizing materials and various articles from these materials. The results described in the paper also provide better understanding of the reasons for various adverse factors distorting the structural homogeneity of these materials.

REFERENCES

1. A. P. Aldushin and A. G. Merzhanov, "Theory of filtration combustion: General notions and state of research," in: Yu. Sh. Matros (ed.), *Propagation of Heat Waves in Heterogeneous Media* [in Russian], Nauka, Novosibirsk (1988), pp. 9–52.
2. A. P. Aldushin, "Filtration combustion of metals," *ibid.*, pp. 52–71.
3. T. P. Ivleva, A. G. Merzhanov, and K. G. Shkadinskii, "Surface combustion of porous condensed substances with condensed products," in: *Chemical Physics of Combustion and Explosion Processes. Combustion of Condensed and Heterogeneous Systems* (collected scientific papers) [in Russian], Chernogolovka (1980), pp. 63–67.
4. V. V. Grachev and T. P. Ivleva, "Two-dimensional modes of filtration combustion," *Combust., Expl., Shock Waves*, **35**, No. 2, 126–132 (1999).
5. S. B. Shcherbak, "Unstable combustion of samples of gas-free compositions in the form of rods of square and circular cross section," *Combust., Expl., Shock Waves*, **19**, No. 5, 542–544 (1983).
6. T. P. Ivleva and A. G. Merzhanov, "Mathematical simulation of three-dimensional spin regimes of gasless combustion," *Combust., Expl., Shock Waves*, **38**, No. 1, 41–48 (2002).
7. A. P. Aldushin and S. G. Kasparyan, "Stability of stationary filtrational combustion waves," *Combust., Expl., Shock Waves*, **17**, No. 6, 615–624 (1981).
8. A. K. Filonenko, "Unsteady processes in combustion of heterogeneous systems yielding high-melting products," in: A. G. Merzhanov (ed.), *Combustion Processes in Chemical Technology and Metallurgy* [in Russian], United Inst. Chem. Phys., USSR Academy of Sci., Chernogolovka (1976), pp. 258–273.
9. A. A. Samarskii, *Theory of Difference Schemes* [in Russian], Nauka, Moscow (1989).
10. T. P. Ivleva and K. G. Shkadinskii, "Algorithm for constructing a moving nonuniform adaptive computational grid," Informational Bulletin of the State Database for Algorithms and Codes of the USSR, No. 1(27), 18–19 (1979).
11. V. A. Vol'pert, A. V. Dvoryankin, and A. G. Strunina, "Non-one-dimensional combustion of specimens with rectangular cross section," *Combust., Expl., Shock Waves*, **19**, No. 4, 377–379 (1983).